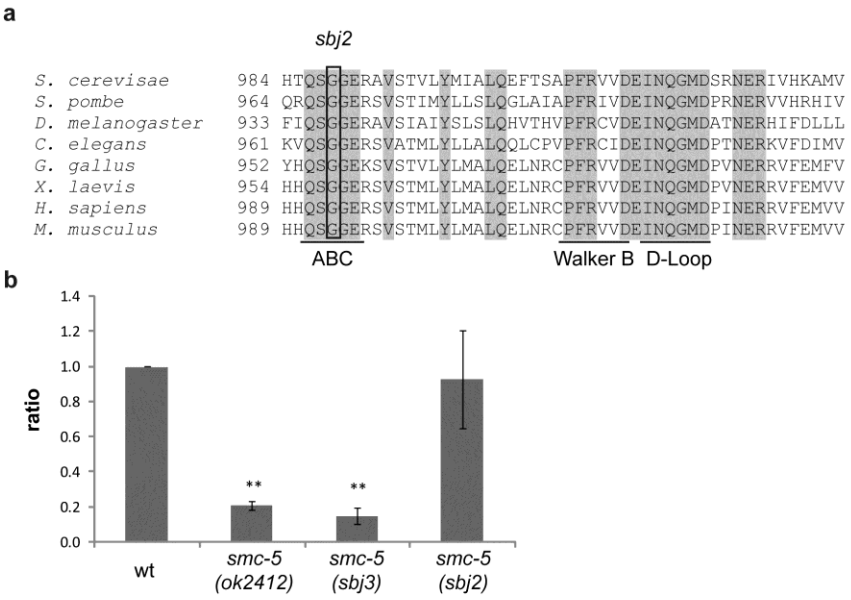

Figure S1 ***sbj2*** **allele of** ***smc-5*** **disrupts the ABC signature motif while** ***sbj3*** **and** ***ok2421*** **have reduced mRNA levels of** ***smc-5*****.** **a.** Alignment of carboxyl-terminal regions of SMC-5 homologs highlighting *sbj2* allele that changes a Glycine (G) of a conserved ABC signature motif into an Arginine (R). **b.** RT qPCR of *smc-5* using populations of mixed stages of the indicated genotypes. Error bars represent standard deviation between three biological replicates. *smc-5* mRNA levels were significantly reduced in *smc-5(ok2421)* and *(sbj3)* but not *(sbj2)* alleles. Double-asterisks (**) denote p value >0.0001 calculated applying two-tailed students T-Test.

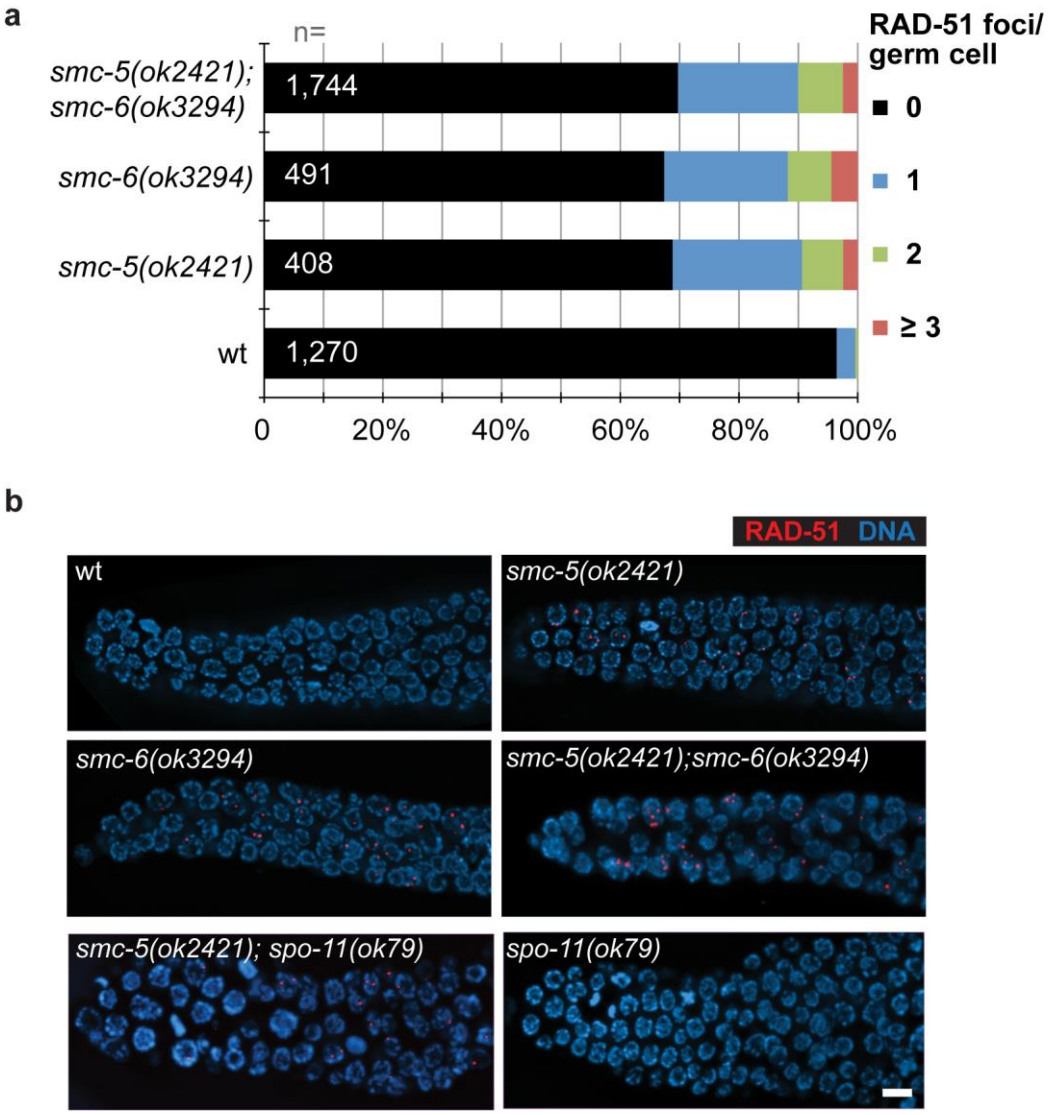

Figure S2 Worms with SMC-5/6 complex defect accumulate RAD-51 foci in mitotic germ cells independently of *spo-11*. **a.** Percentages of germ cells in L4 larval mitotic germline containing 0, 1, 2, 3 or more RAD-51 foci per nucleus. The number of germ cells quantified for each genotype is indicated at the base of the bars. The graph is based on αRAD-51 and DAPI staining of dissected germlines. **b.** αRAD-51 and DAPI staining of dissected germline. Shown are representative deconvolved images of young adults for *smc-5(ok2421);spo-11(ok79)* and *spo-11(ok79)*, and the rest are of L4 larvae. Scale bar = 5 µm.

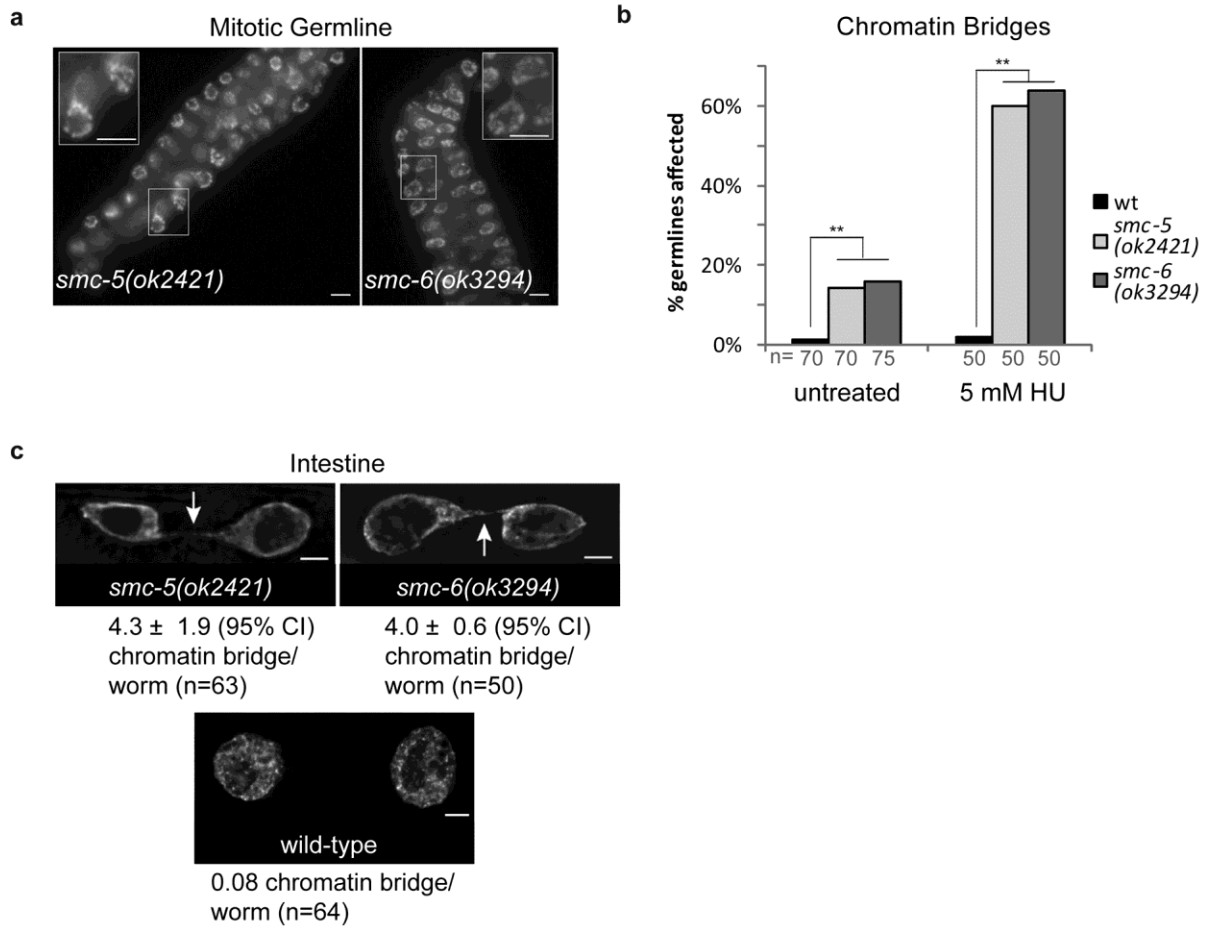

Figure S3 Loss-of-function mutations in *smc-5* and *smc-6* confer a chromatin-bridging defect in the L4 larval germline.
a. DAPI staining of dissected L4 larval germ cells. A magnified view of DNA bridges in the respective germline is depicted in the inset image. **b.** Graph showing the percentage of germlines containing one or more chromatin bridges for untreated and 5mM hydroxyurea (HU) treated L4 larvae. Double asterisks represent p value <0.01 in comparison to wild-type. Statistical analyses used the two-tailed Fisher's Exact Test comparing the total number of affected and unaffected germlines. **c.** DAPI staining of dissected adult intestine with quantification of chromatin bridges observed in *smc-5* and *smc-6* mutants compared to wild-type. Scale bars = 5 µm.

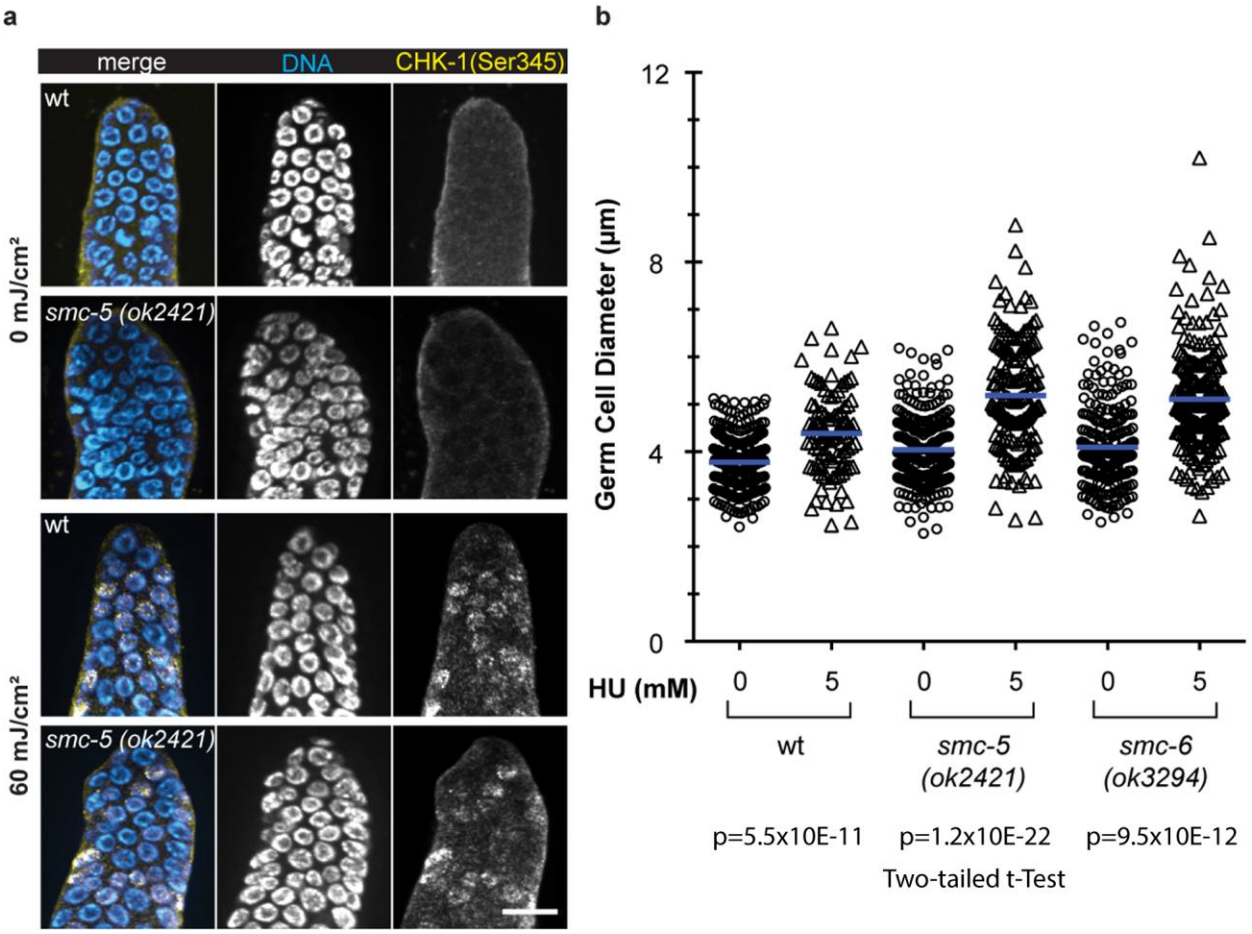

Figure S4 DNA damage checkpoint could be induced in *smc-5* and *-6* mutant worms similar to wild-type.
a. Immunostaining of Serine 345-phosphorylated CHK-1 and DAPI staining of DNA in the proliferative zone of germline in young adult worms. Germlines were dissected 30 min after irradiation with 60 mJ/cm² UVB. Untreated samples were collected in parallel. Shown are representative images. Scale bar = 10 µm. **b.** The scatter plot shows the nuclear diameter of germ cells ± HU treatment (n≥260 nuclei from 13 or more germlines per condition). The mean diameters are represented by the blue lines.

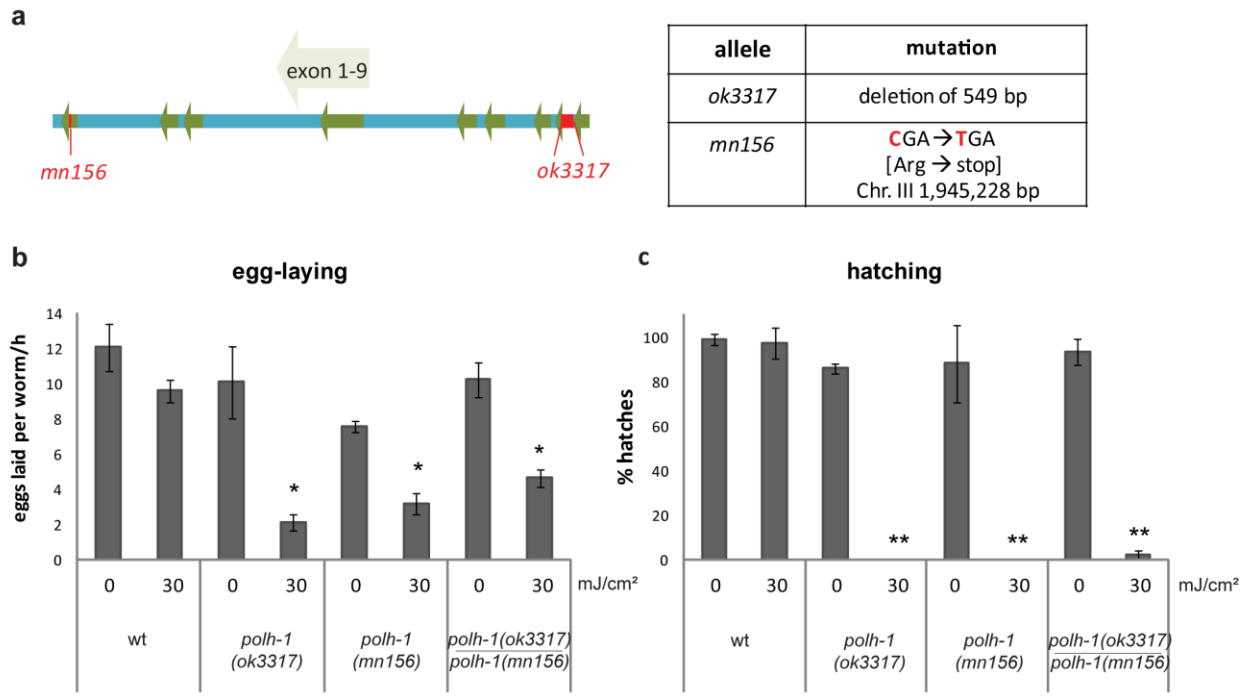

allele	mutation
ok3317	deletion of 549 bp
mn156	CGA→TGA [Arg → stop] Chr. III 1,945,228 bp

Figure S5 ***mn156* is a nonsense mutation in *polh-1*.**
a. Genomic locus of *polh-1* (III: 1,945,111bp – 1,950,257bp) with exon location and annotation of *mn156* and *ok3317* alleles. **b.** Eggs laid 24h post irradiation at L4 stage. Shown are averages between three replicates of three worms. Error bars indicate standard deviation between the replicates. **c.** Percentage of hatches two days after egg-laying. Displayed are averages between three replicates of three worms. Error bars indicate standard deviation between the independent replicates.

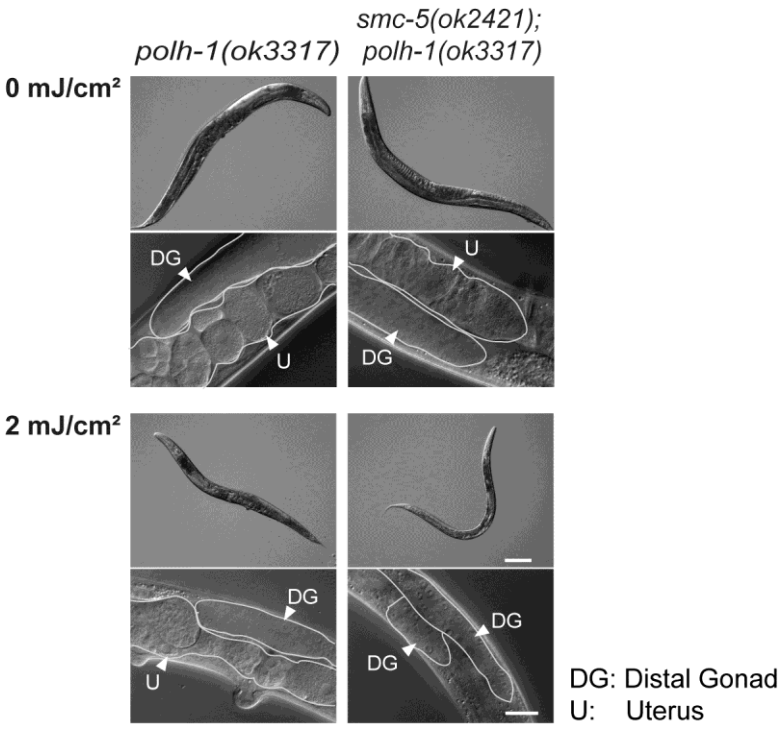

Figure S6 ***smc-5;polh-1*** **double mutants are impaired in somatic tissues and germline after UVB irradiation.**
DIC images of whole worms and magnified view of mid-body 72h after L1 stage. Synchronized worms were irradiated at L1 larval stage and maintained at 20 °C. Scale bar = 100 µm (upper panels) and 20 µm (lower panels). Shown are *polh-1(ok3317)* and *polh-1(ok3317);smc-5(ok2421)* mutant strains that were treated and analyzed in parallel to worms depicted in Figure 4.

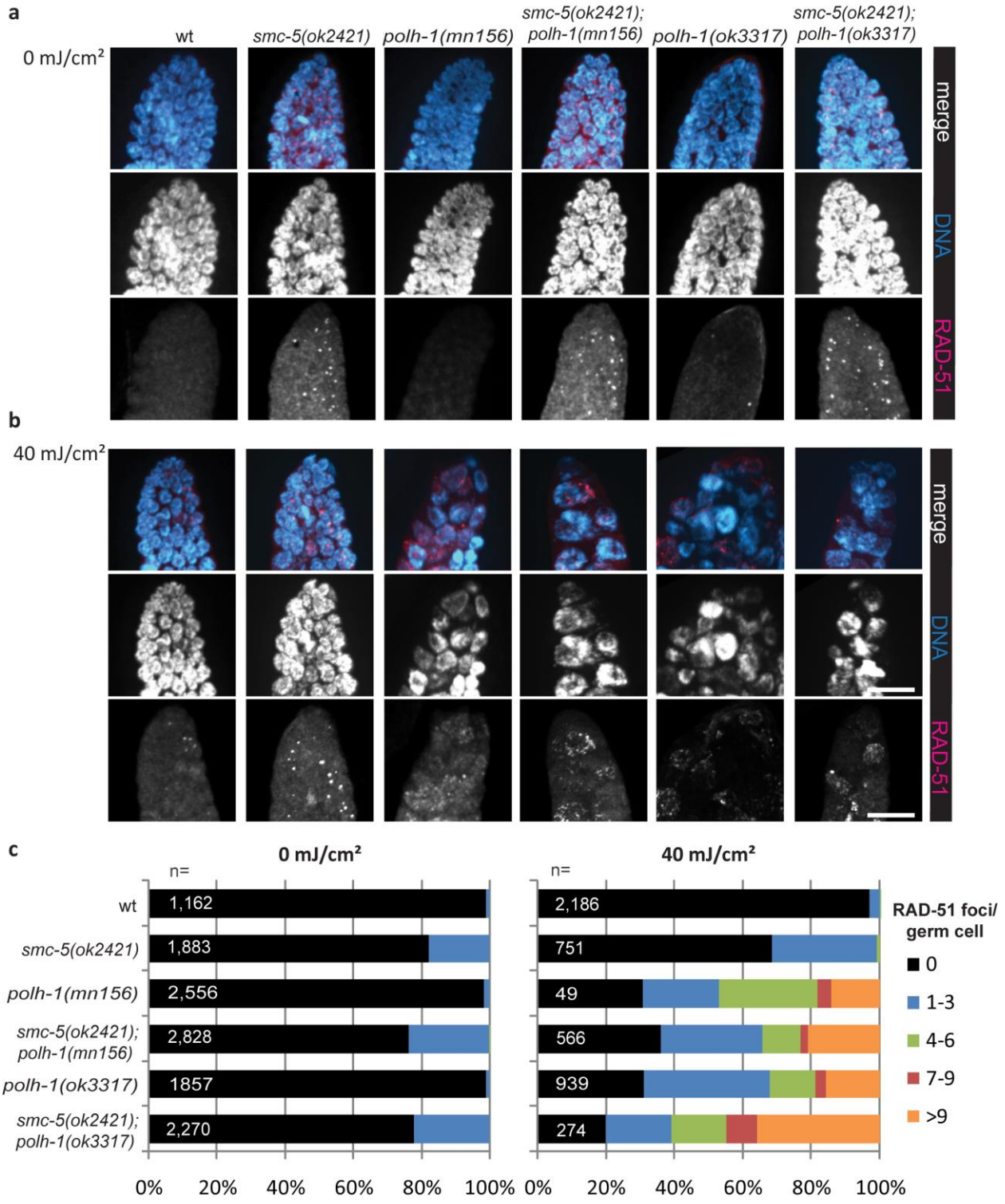

Figure S7 ***polh-1*** **mutant germ cells arrest upon UVB irradiation and display DNA bridges.**
a. and b. αRAD-51 and DAPI staining of mitotic germ cells. Young adults were dissected 24 h after UVB irradiation (**b**) and untreated controls were dissected in parallel (**a**). Representative images in extended view of stack spanning the whole germline are shown. Scale bar = 10 µm. **c.** Percentages of germ cells in L4 larval mitotic germline containing 0, 1-3, 4-6, 7-9, and more than 9 RAD-51 foci per nucleus. The number of germ cells quantified for each genotype is indicated at the base of the bars. The graph is based on αRAD-51 and DAPI staining of dissected germlines.

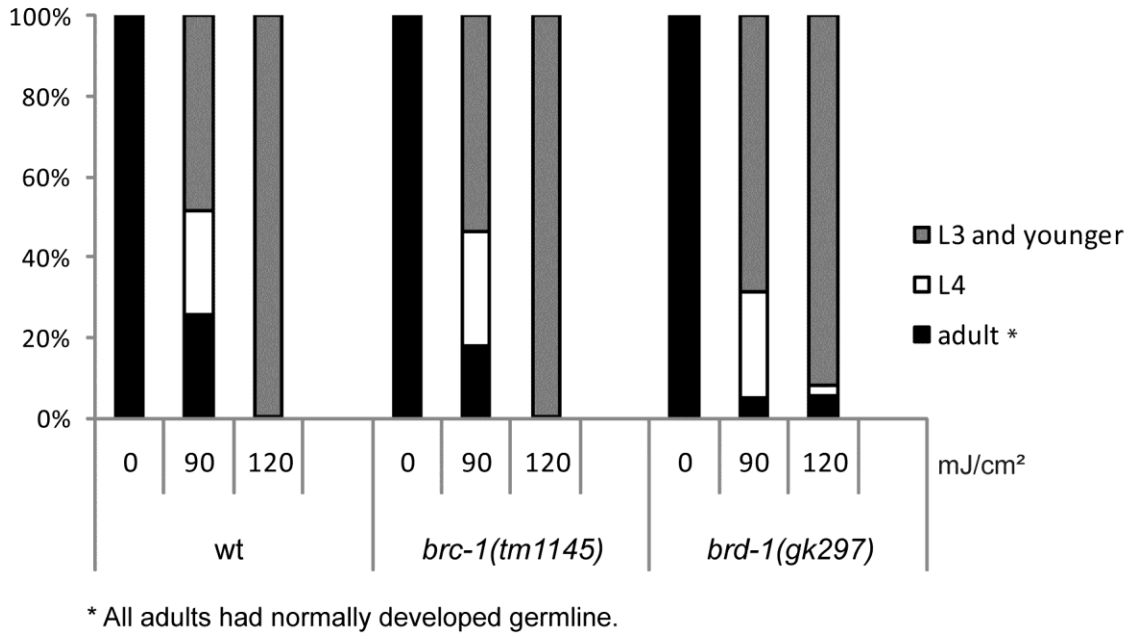

Figure S8 ***C. elegans*** **with disrupted BRC-1/BRD-1 complex are as sensitive to UVB irradiation as wild-type worms.** Percentage of larval stages 72h after UVB irradiation at L1 larval stage of the indicated genotypes.

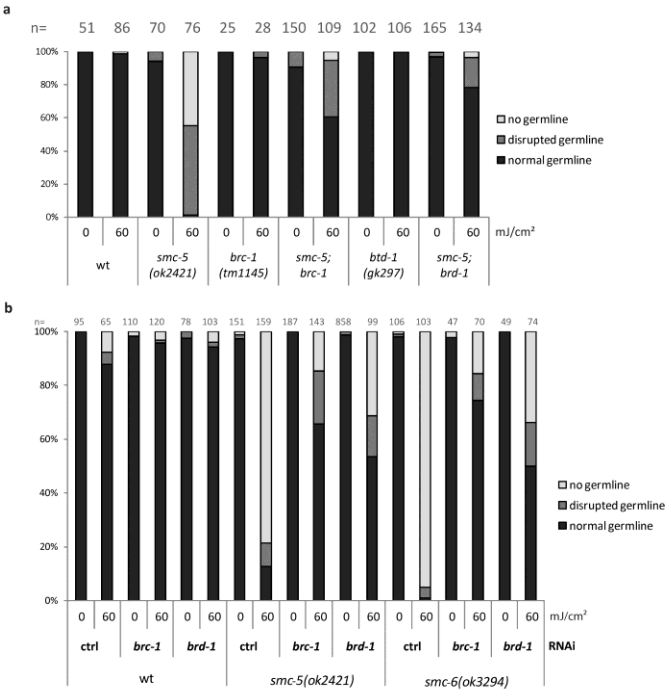

Figure S9 *brd-1* and *brc-1* inactivation rescues UV hypersensitivity of *smc-5* and *smc-6* mutants.
a. Quantification of germline development of worms three days after irradiation with UVB at L1 stage or untreated control worms. Worms were categorized into groups of 'normal', 'disrupted' and 'no germline' by inspection on a dissection microscope. **b.** L4 larvae were placed on the indicated RNAi bacteria and F1 generation was bleached. F2 worms were irradiated and raised on the same RNAi bacteria as the F1 was grown on. As read-out worms were categorized into groups of 'normal', 'disrupted' and 'no germline' by inspection on a dissection microscope. Graph shows germline development quantification of worms three days after irradiation with UVB at L1 stage or untreated control worms. n indicates number of animals assessed, representative experiment shown.

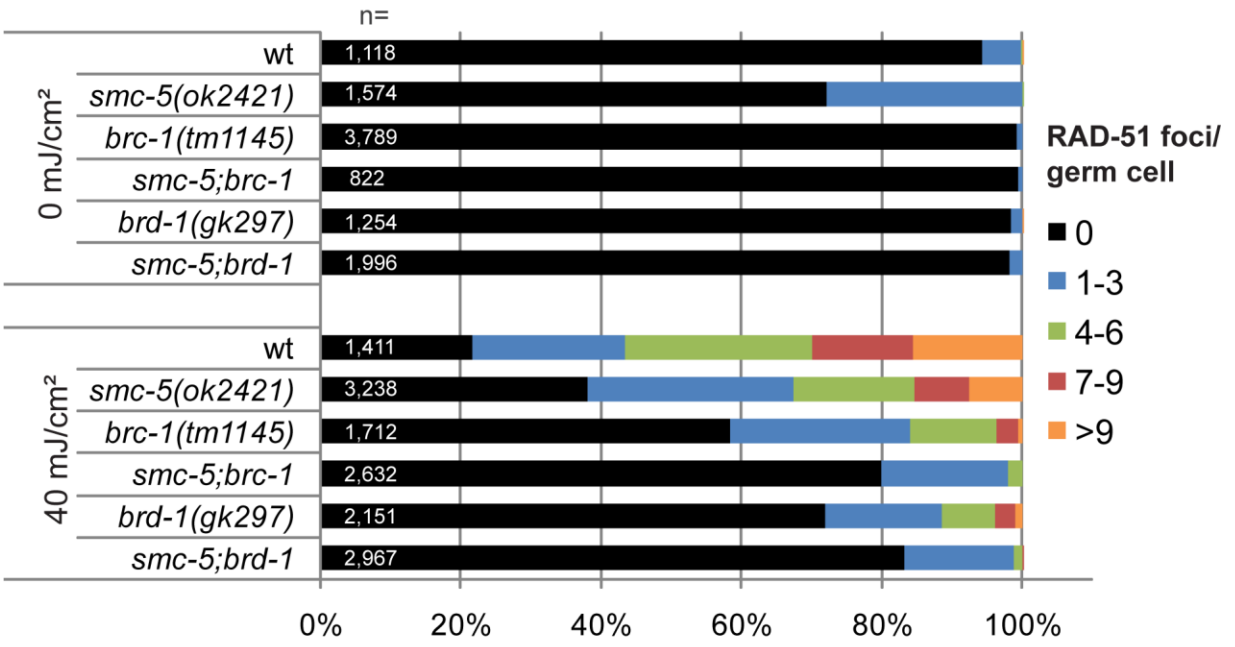

Figure S10 Quantification of RAD-51 foci that are representatively shown in Figure 6A.
Percentages of germ cells in L4 larval mitotic germline containing 0, 1-3, 4-6, 7-9, and more than 9 RAD-51 foci per nucleus. The number of germ cells quantified for each genotype is indicated at the base of the bars. The graph is based on αRAD-51 and DAPI staining of dissected germlines.

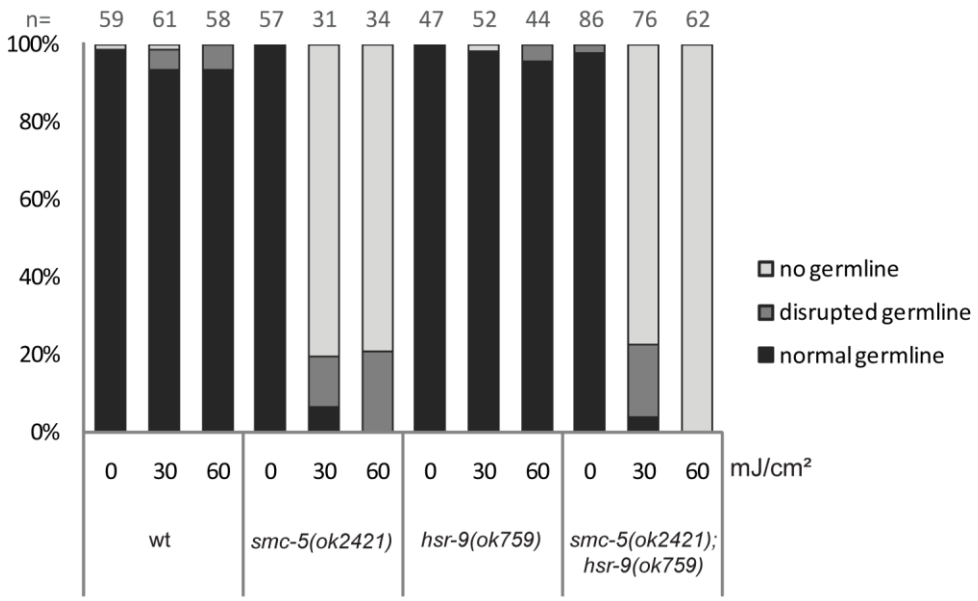

Figure S11 ***hsr-9*** **is dispensable for germline development upon UV irradiation and does not genetically interact with** ***smc-5*****.** Quantification of germline development of worms three days after irradiation with UVB at L1 stage or untreated control worms. Worms were categorized into groups of 'normal', 'disrupted' and 'no germline' by inspection on a dissection microscope. n indicates number of animals assessed, representative experiment shown.

Table S1 List of *C. elegans* strains used in the study.

Strain	Genotype
BJS21	*csb-1(ok2335) X; xpc-1(tm3886) IV.*
BJS78	*smc-5(sbj3))/mln1[mls14 dpy-10(e128)] II.*
BJS79	*smc-5(sbj2))/mln1[mls14 dpy-10(e128)] II.*
BJS99	*smc-5(ok2421))/mln1[mls14 dpy-10(e128)] II ; csb-1(ok2335) X.*
BJS101	*smc-5(ok2421))/mln1[mls14 dpy-10(e128)] II ; xpc-1(tm3886) IV.*
BJS121	*smc-5(ok2421))/mln1[mls14 dpy-10(e128)] II ;brd-1(gk297) III.*
BJS123	*smc-5(ok2421))/mln1[mls14 dpy-10(e128)] II ;brc-1(tm1145) III.*
BJS125	*smc-5(ok2421))/mln1[mls14 dpy-10(e128)] II ; hsr-9(ok759) I.*
BJS127	*smc-5(ok2421))/mln1[mls14 dpy-10(e128)] II ; div-1(or148) III.*
BJS144	*smc-5(ok2421))/mln1[mls14 dpy-10(e128)] II; polh-1(ok3317) III.*
BJS146	*smc-5(ok2421))/mln1[mls14 dpy-10(e128)] II; polh-1(mn156) III.*
DW102	*brc-1(tm1145) III.*
EU548	*div-1(or148) III.*
FX03886	*xpc-1(tm3886) IV.*
N2	wild-type.
RB1801	*csb-1(ok2335) X.*
SP488	*rad-2(mn156) III.*
VC573	*hsr-9(ok759) I.*
VC655	*brd-1(gk297) III.*
XF656	*polh-1(ok3317) III.*
YE35	*smc-5(ok2421)/mln1[mls14 dpy-10(e128)] II;spo-11(ok79) IV/nT1[unc-?(n754) let-?] IV;V.*
YE57	*smc-5(ok2421)/mln1[mls14 dpy-10(e128)] II.*
YE58	*smc-6(ok3294)/mln1[mls14 dpy-10(e128)] II.*

Table S2 Validation of statistical significance applying χ^2 and two-tailed Fisher's Exact Test for germline development determined in this study.

Available for download as an Excel file at http://www.genetics.org/lookup/suppl/doi:10.1534/genetics.113.158295/-/DC1